Histol Histopathol (2016) 31: 1089-1094

http://www.hh.um.es

Histology and Histopathology

From Cell Biology to Tissue Engineering

Atrophic hepatocytes express keratin 7 in ischemia-associated liver lesions

Ioanna Delladetsima[1], Stratigoula Sakellariou[1], Aikaterini Kokkori[1,3] and Dina Tiniakos[2,4]

[1]First Department of Pathology and [2]Laboratory of Histology-Embriology, Medical School, National and Kapodistrian University of Athens, Athens, Greece, [3]Institute of Pathology and Molecular Pathology, Helios Klinikum Wuppertal, Germany and [4]Institute of Cellular Medicine, Faculty of Medical Sciences, Newcastle University, UK

Summary. Aim: To investigate atrophic parenchymal changes in ischemic liver conditions. Design: We studied 18 cases of hepatic lesions with atrophic changes due to altered blood flow (hepatic venous congestion n=15 including 4 cases with additional nodular regenerative hyperplasia-NRH, NRH n=1, and antiphospholipid syndrome with patchy parenchymal atrophy n=2). Metaplastic hepatocellular changes, hepatocyte proliferation, hepatic stellate cell (HSC) activation, and sinusoidal capillarization were examined immunohistochemically with antibodies to keratins (K) 7 and 19, Ki67, αSMA and CD34, respectively. Results: K7 was positive and K19 was negative in zone 3 atrophic hepatocytes in venous congestion and in areas of plate atrophy, as well as in congested or compressed sites in NRH. Sinusoidal CD34-positivity indicating capillarization accompanied K7 immunoexpression. Masson trichrome revealed sinusoidal fibrosis to be restricted in atrophic areas, usually mild and in 7 cases focally dense. αSMA expression expanded beyond K7-positive areas. Ki67 was negative in K7-positive hepatocytes. Conclusion: Ischemic parenchymal changes are characterized by hepatocyte K7 immunoexpression, sinusoidal capillarization, HSC activation and lack of cellular proliferation, indicating an early reaction of the major liver parenchyma cellular components creating a more resistant microenvironment. These phenotypic alterations may prove valuable in the discrimination of ischemic liver lesions.

Offprint requests to: Dr Ioanna Delladetsima, First Department of Pathology, Medical School, University of Athens, Athens, M. Asias 75, Goudi, Athens, 11527 Greece. e-mail: jokadelladetsima@hotmail.com

DOI: 10.14670/HH-11-738

Key words: Liver, Ischemia, Hypoxia, Keratin 7, Congestion, Nodular regenerative hyperplasia

Introduction

Hypoxia across the hepatic acinus has profound effects on functional and structural integrity of the liver parenchyma. It not only affects hepatocytes, but also partner cells such as hepatic stellate cells (HSC) and endothelial cells. There are ultrastructural changes (Józsa et al., 1981; Phillips, 1987; Schön et al., 1998) indicating successive hepatocellular injury appearing already at the very early stage, while both molecular and translational findings from *in vitro* studies provide evidence of hypoxia-induced HSC activation and fibrogenic and angiogenic stimuli (Nath and Szabo, 2012). Additionally, protective mechanisms based on the plasticity of hepatocytes are thought to exist as an attempt at phenotypic and functional accommodation to an unfavorable microenvironment (Delladetsima et al., 1995, 2010; Desmet, 2011a,b).

Hypoxia is pathogenetically implicated in various liver lesions. Representative forms, besides ischemic necrosis, are hepatocyte atrophy associated with venous stasis, atrophy without evidence of congestion, atrophy combined with regeneration as in nodular regenerative hyperplasia (NRH), and preservation–reperfusion injury in liver grafts. Venous stasis as a result of venous outflow impairement irrespective of etiology is histologically characterized by congestion and dilatation of sinusoids in parallel with atrophy of hepatocyte plates. In mild forms there is minimal sinusoidal fibrosis while severe fibrosis with collagenization of sinusoids

appears in advanced atrophy with hepatocyte loss (Wanless and Huang, 2011; Krings et al., 2014). Atrophy without fibrosis or with mild sinusoidal fibrosis is encountered in portal vein thrombosis (Wanless and Huang, 2011) and in the liver parenchyma adjacent to expanding regenerative nodules in NRH (Stromeyer and Ishak, 1981; Wanless, 1990). Information regarding subtle parenchymal alterations in lesions associated with diminished blood supply is limited and based mainly on morphology.

In the present study, we investigated immunophenotypic alterations of hepatocytes, HSC and sinusoidal endothelial cells in hypoxic/ischemic conditions in order to gain insight into early parenchymal histological reactions and their possible diagnostic significance.

Materials and methods

We selected from the archives of the 1st Department of Pathology and the Laboratory of Histology-Embryology University of Athens 18 anonymised liver disease cases with mild ischemic histological changes from 11 male and 7 female patients with mean age 62 years (range 34-75 years). These included twelve liver core needle biopsies (each >1.5cm long with >12 portal tracts) showing either venous congestion (n=7), venous congestion and additional NRH (n=3) or areas of hepatocyte plate atrophy (n=2, antiphospholipid syndrome). The thirteenth and fourteenth case were wedge liver biopsies diagnosed as NRH and venous congestion with concomitant findings of NRH, respectively. The 4 remaining cases were liver lobectomies (3 for HCC and 1 for hepatocellular adenoma) with areas of venous congestion due to tumor mass effect in the background non-cirrhotic liver. Table 1 summarises patient demographics, clinical history, diagnosis and histological findings of each case. These cases were selected because they did not show any additional necroinflammatory or cholestatic changes following careful histological examination while fibrosis was absent or was thin septal in Haematoxylin–Eosin (H&E) staining. Normal liver tissue sections at a distance from the tumor mass in the lobectomy cases served as negative control.

All specimens were fixed in 10% neutral formalin solution and processed according to routine protocols. Paraffin sections stained with H&E, Masson trichrome (MT) and Gomori were re-evaluated by two experienced liver pathologists. Sinusoidal fibrosis was assessed as mild when evident only in MT stained sections and dense when detected on H&E (Brunt et al., 2012).

Paraffin-embedded 4 μm-thick serial sections were cut for immunohistochemical analysis. Immunostaining for keratin 7 (anti-keratin 7 antibody OV-TL12/30, dilution 1:500, Dako, Carpinteria, CA) and keratin 19 (anti-keratin 19 antibody RCK108, dilution 1:200, Dako, Carpinteria, CA) was performed to highlight metaplastic hepatocellular changes and ductular reaction (DR) while αSMA (anti-alpha smooth muscle actin antibody 1A4, dilution 1:800, Dako, Carpinteria, CA) was used as a marker for activated HSC. Capillarization of sinusoids was examined using an anti-CD34 antibody (QBEnd 10, 1:300, Dako, Carpinteria, CA) and proliferation of hepatocytes was evaluated based on Ki67 (clone MIB-1, 1:200, Dako, Carpinteria, CA) labeling index. The two-step peroxidase conjugated polymer technique (DAKO Envision kit, DAKO, Carpinteria, CA) was applied according to the manufacturer's instructions. 3'3-diaminobenzidine was used as chromagen.

Evaluation of immunostaining was performed by two expert liver pathologists at a double-headed microscope. All markers were evaluated based on cell type stained and acinar distribution pattern. Recognition of zone 1 and 3 was based on their topographical relationship with the anatomic units, portal tracts and terminal hepatic venules and thus permitted a vague discrimination of the intermediate zone 2. Keratin 7 (K7) and keratin 19 (K19) immunoreactivity was assessed based on immunostaining intensity (3-tier system, grade 0-2, where grade 2 is the staining intensity of normal interobular bile duct cells, grade 1 any positive immunostain milder than grade 2, and 0 absence of K7- or K19-immunoreactivity). A quantitative assessment of grade 2 and grade 1 K7-positive hepatocytes has additionally been performed.

Results

K7 was positive in zone 3 atrophic hepatocytes in all cases of venous congestion (Fig. 1). K7 expression was also observed in atrophic hepatocytes in congested or compressed sites at the periphery of regenerative nodules in NRH (Fig. 2) as well as in areas of small-sized hepatocytes consistent with patchy parenchymal atrophy in cases of antiphospholipid syndrome (Fig. 3). K7 immunostaining was stronger (grade 2) in congested zone 3 hepatocytes compared to less intensively stained (grade 1) atrophic hepatocytes at the periphery of NRH and in sites of patchy atrophy. K7 immunostaining intensity grading for each case is described in Table 1. In all cases, CD34 showed linear endothelial immunostaining along sinusoids with a distribution pattern similar to that of K7 (Figs. 2, 3). MT staining revealed sinusoidal fibrosis to be restricted in areas of K7 positivity. Sinusoidal fibrosis was mild and in 7 cases was focally dense. αSMA-immunoreactive HSC expanded beyond the atrophic K7-positive areas in declining density (Fig. 3). In serial sections examined, Ki67 was negative in K7-positive hepatocytes while proliferation was detectable in a small number of hepatocytes in the adjacent non-congested parenchyma. K19 immunostaining was absent in K7-positive areas while dense cytoplasmic K19 positivity highlighted interlobular bile ducts and ductules. Mild DR positive for K7 and K19 was occasionally encountered periportally. In 3 cases, a few ductular structures were topographically associated with atrophic zone 3 K7-

positive hepatocytes. There were no abnormal immunohistochemical findings in the control liver sections. Immunohistochemical findings (acinar topography and extent of immunoreactivity) regarding K7, CD34 and αSMA expression as well as perisinusoidal fibrosis are shown in detail in Table 1.

Table 1. Summarises patient demographics, clinical history, diagnosis, histological and immunohistochemical findings and their acinar distribution in every case.

Gender/Age (years-y) Specimen type	Clinical History	Diagnosis	Histological features, Acinar topography and extent (% of acini)	K7+ hepatocytes Acinar topography, immunostaining intensity (Grade 1-2, G1-2), and % of K7+ hepatocytes with G1 or G2	CD34+ Acinar topography	aSMA+ Acinar topography	Perisi-nusoidal fibrosis in atrophic areas (MT)
1. M/73 Core biopsy	Heart Failure	Hepatic venous congestion	SD & PA Z3 & Z2 80%	Z3 & Z2 G2 80%, G1 20% DS	As K7	Panacinar	Mild, focally dense
2. F/47 Core biopsy	Right atrial myxoma	Hepatic venous congestion	SD & PA Z3 70%	Z3 G2 60%, G1 40%	As K7	Z3 & Z2	Mild
3. M/50 Core biopsy	Non neoplastic solitary cyst	Hepatic venous congestion	SD & PA Z3 60%	Z3 G2 50%, G1 50%	As K7	Z3 &Z2	Mild
4. F/75 Core biopsy	Heart failure	Hepatic venous congestion	SD & PA Z3 & occasionally Z2 70%	Z3+occasionally Z2 G2 75%, G1 25%	As k7	Panacinar	Mild, focally dense
5. M/72 Core biopsy	Right hepatic vein thrombosis Polycythemia	Hepatic venous congestion & early NRH	SD & PA Z3 & Z2 70% Few poorly discernible RN	Z3+ occasionally Z2 G2 60%, G1 40% Segmentally at the RN periphery G2 20%, G1 80%	As k7	Panacinar	Mild, focally dense
6. F/68 Core biopsy	Colorectal Ca 3 liver lesions	Hepatic venous congestion	SD & PA Z3 40%	Small number of HC in Z3 G2 80%, G1 20%	Small number of EC	Z3 & Z2	Focally mild
7. M/54 Core biopsy	LT 15y ago No immunosuppression Pulmonary hypertension	Hepatic venous congestion	SD & PA Z3 60%	Z3 G2 75%, G1 25%	More diffuse than K7, Higher density in Z3	Z3 & Z2	Mild
8. F/72 Core biopsy	Heart failure	Hepatic venous congestion & early NRH	SD & PA Z3 50% Few poorly discernible RN	Z3 G2 35%, G1 65% Segmentally at the RN periphery: G2 30%, G1 70%	As K7	Panacinar More dense in atrophic areas	Mild
9. M/68 Core biopsy	Heart failure	Hepatic venous congestion + early NRH	SD & PA 50% Few poorly discernible RN	Z3 G2 50%, G1 50% Segmentally at the RN periphery: G2 50%, G1 50%	As K7	Panacinar Lower density in Z1	Mild and focally dense
10. M/39 Core biopsy	Hypercoagulable state	Budd-Chiari Hepatic venous congestion	SD & PA Z3 100%	Z 3 and Z 2 G2 90%, G1 10% DS	As K7	Panacinar More dense in atrophic areas	Mild, focally dense
11. M/67 Core biopsy	SLE & anti-phospholipid syndrome	PA	Irregular atrophic areas, no zonal distribution	Limited to atrophic areas G2 35%, G1 65%	As K7	Panacinar, More dense in atrophic areas	Mild
12. F/46 Core biopsy	RA & anti-phospholipid syndrome	PA	Irregular atrophic areas no zonal distribution	Limited to atrophic areas G2 40%, G1 60%	As K7	Panacinar	Mild
13. M/65 Wedge biopsy	Cholecystectomy Mild PV dilatation	NRH	RN	Segmentally at the periphery of RN G1 100%	Small number of EC in K7+ areas	Limited to atrophic areas	No fibrosis
14. M/70 Wedge biopsy	Liver mass	Hepatic venous congestion & NRH	SD & PA Z3 60% Recognizable RN	Z3 G2 60%, G1 40% Segmentally at the RN periphery G2 50%, G1 50% DS	As K7	Panacinar	Mild
15. M/69 Lobectomy	Liver mass	HCC & Hepatic venous congestion	SD & PA Z3 80%	Z3+occasionally Z2 G2 80%, G1 20%	As K7	Z3 & Z2	Mild, focally dense in AA
16. F/35 Lobectomy	Liver mass	HCA & Hepatic venous congestion	SD & PA Z3 60%	Z3 G2 60%, G1 40%	As K7	Z3 & Z2	Mild
17. F/75 Lobectomy	Liver mass	HCC & Hepatic venous congestion	SD & PA Z3 70%	Z3 G2 75%, G1 25%	As K7	Panacinar	Mild, focally dense
18. M/72 Lobectomy	Liver mass	HCC & Hepatic venous congestion	SD & PA Z3 60%	Small number of HC in Z3 G2 50%, G1 50%	As K7	Panacinar, More dense in atrophic areas	No fibrosis

DS, Ductular Structures; EC, Endothelial Cells; F, Female; G, Grade of immunohistochemical intensity; HC, Hepatocytes; K7, Keratin 7; LT., Liver Transplantation; M, Male; MT, Masson trichrome; NRH, Nodular Regenerative Hyperplasia; PA, Plate Atrophy; PSF, Perisinusoidal Fibrosis; PV, Portal Vein; RA, Rheumatoid Arthritis; RN, Regenerative Nodules; SD, Sinusoidal Dilatation; SLE, Systematic Lupus Erythematosus; T, Acinar topography; Y, years; Z, Zone.

Discussion

Our findings revealed that diminished blood supply affects the main cellular components of liver parenchyma. The most interesting observation was the alteration of hepatocyte immunophenotype characterized by the expression of K7 in atrophic less oxygenated areas. K7-positive hepatocytes were observed in congested zone 3 in cases with venous stasis, in compressed atrophic plates in NRH, and in patchy parenchymal atrophy in the absence of adjacent hepatic progenitor cells and/or ductular structures, while mild DR was occasionally seen periportally. The presence of K7-positive hepatocytes as a characteristic finding in various ischemia related conditions has not been previously noted. It was implied in the past in the context of DR type 2B described by Desmet (2011a,b) and has recently been demonstrated by Krings et al in cases of venous outflow obstruction in association with zone 3 DR (Krings et al., 2014). In addition, K7 immune reactivity in zone 3 was also observed in the majority of liver biopsies from patients with heart failure extending

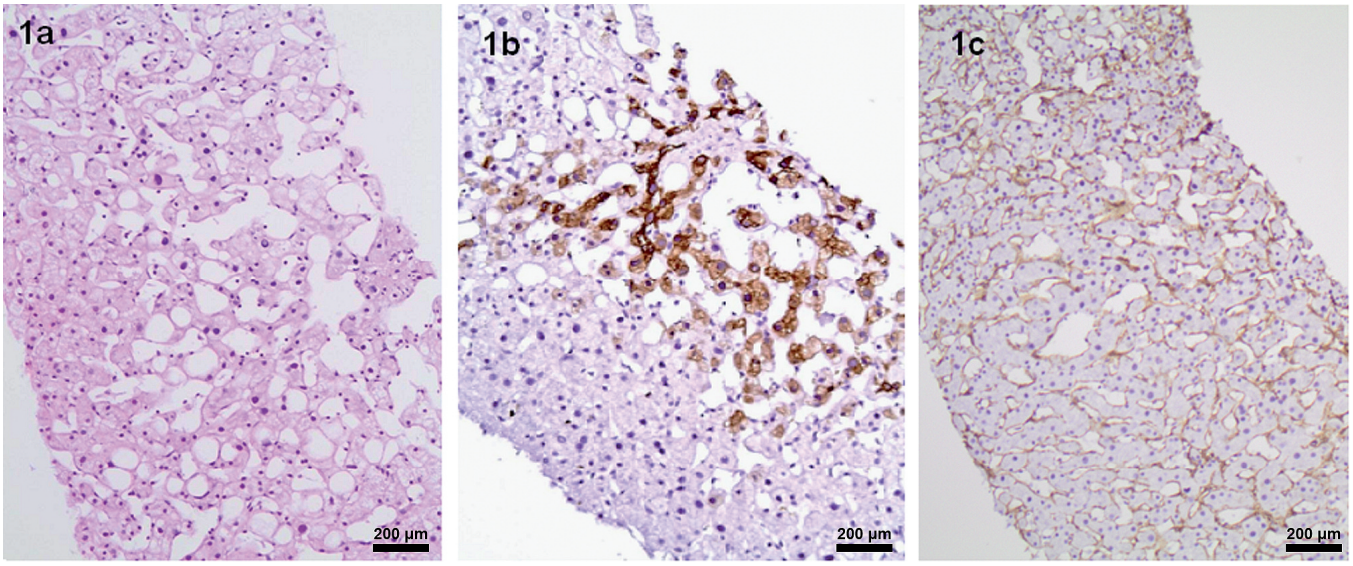

Fig. 1. Zone 3 "atrophic" hepatocytes in a case of venous congestion. K7 positivity indicates stasis versus an "artifact". αSMA expression expanding beyond zone 3. a, H&E; b, K7; c, αSMA. x 20

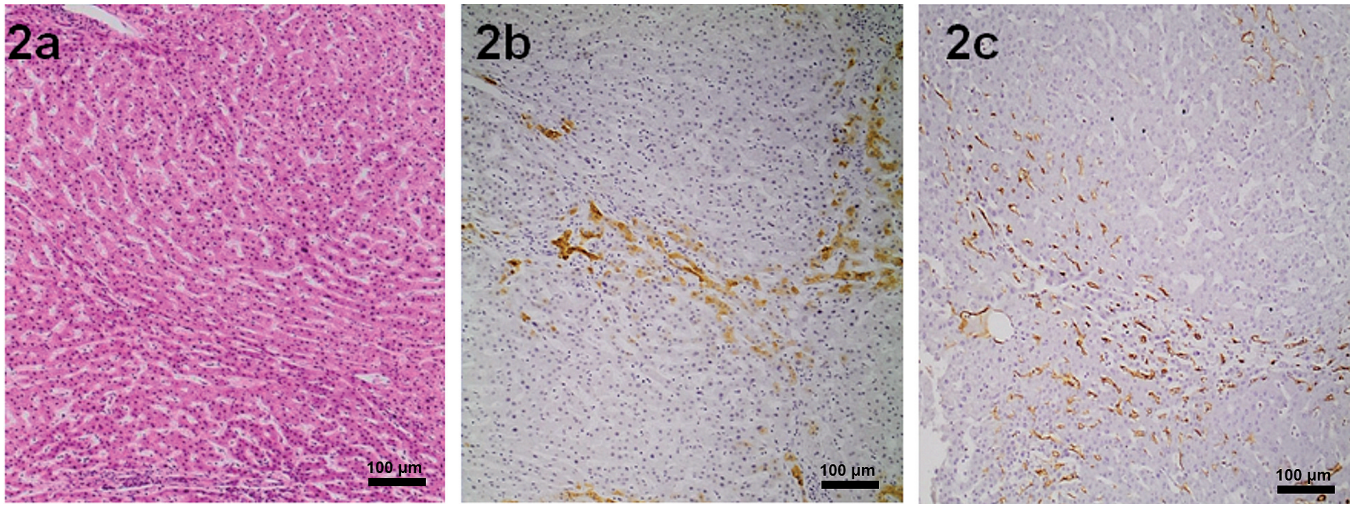

Fig. 2. Compressed atrophic plates at the periphery of regenerative nodules (H&E) **(a)**, positive for K7 **(b)**. Capillarization of sinusoids at the same area (CD34) **(c)**. x 10

into zone 2 in parallel with fibrosis in more severe cases (Pai and Hart, 2010).

DR type 2B is thought to be hypoxia-induced occurring in zone 3 of liver acini (Desmet, 2011a,b; Krings et al., 2014) and in the cirrhotic nodules (Desmet, 2011a,b), while Pai and Hart (2010) postulated an aetiological relation to cholestatic injury. The pathogenetic concept relies on a metaplastic or dedifferentiation process leading mature hepatocytes through successive phases to ductule formation. Our findings provide evidence in support of the above hypothesis revealing that K7 hepatocellular immunostaining is an early recognizable immuno-phenotypic alteration due to diminished blood supply and hypoxia-induced parenchymal injury, intimately associated with atrophic changes and irrespective of the ischemic cause. The absence of DR in congested zone 3 in our examined material may be attributed to earlier and milder lesions with no established fibrosis compared to the reported cases in the literature.

K7-positive or intermediate hepatocytes are a well known manifestation of chronic cholestasis. They are primarily located periportally or periseptally and constitute an early sign of a metaplastic or dedifferentiation process which leads to the formation of ductules described as DR type 2A by Desmet (2011a,b). K7-positive hepatic cords evolving to ductular structures have been described in massive and submassive necrosis (Delladetsima et al., 2010) while K7-positive hepatocytes have been observed in cases of chronic hepatitis C, occasionally co-existing with hepatic progenitor cells (Delladetsima et al., 2010). K7 positive centrilobular hepatocytes have been encountered in a variety of liver diseases, but in contrast to our ischemic cases, they appeared singly or in clusters, usually combined with centrilobular scarring and K7-positive periportal hepatocytes (Matsukuma et al., 2012). These trans-differentiation changes, inherent to the plasticity of hepatocytes, possibly represent a protective reaction either to intracellular ingredients such as bile constituents or to adverse extracellular factors (Michalopoulos et al., 2005; Desmet, 2011a,b). In our study, the occurrence of K7-positive atrophic hepatocellular cords in conjunction with ischemic conditions may reflect a phenotypic alteration under the pressure for optimal hepatocellular adjustment to a hypoxic microenvironment. Moreover, the lack of proliferation activity of K7-positive hepatocytes in contrast to neighboring cells may be due to functional deficiency or an energy-sparing cell state.

Our results support hypoxia-induced activation of HSC displayed by αSMA expression. Activated αSMA-positive HSC did not show a strict spatial relationship to the less oxygenated areas, but expanded to parenchymal zones with no morphological or metaplastic hepatocellular alterations, implying a higher sensitivity to low oxygen supply. Convincing evidence of HSC activation derives from experimental studies which disclose the crucial role of hypoxia-inducible factors (HIFs) as homeostatic regulators in almost all cells and tissues under hypoxia, including the liver (Cannito et al., 2014). HIFs are incriminated for the up-regulation of hypoxia response genes coding pro-angiogenic and pro-fibrotic mediators (Copple et al., 2009; Nath and Szabo, 2012; Cannito et al., 2014).

We observed CD34 immunostaining in sinusoidal endothelial cells in association with plate atrophy, K7 hepatocellular expression and mild sinusoidal fibrosis. CD34 sinusoidal expression consistent with capillarization most probably represents an additional microenvironmental phenomenon induced by hypoxia. The susceptibility of endothelial cells is well demonstrated in studies of preservation/reperfusion injury (Hübscher and Clouston, 2011) while zone 3

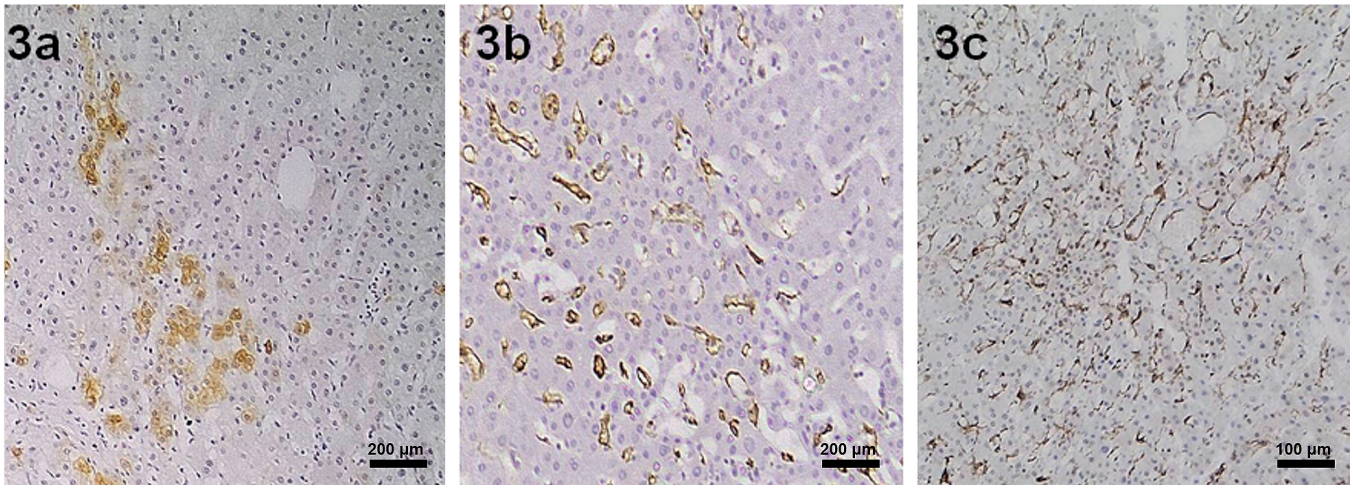

Fig. 3. Small "atrophic" K7-positive hepatocytes **(a)** accompanied by capillarization (CD34) **(b)** and hepatic stellate cell activation (αSMA) **(c)**. a, b, x 20; c, x 10

capillarization has been described in venous outflow obstruction (Krings et al., 2014). Capillarization may precede and probably participates in the process of fibrogenesis (DeLeve, 2007). Our findings allow us to speculate that capillarization constitutes an early event in ischemic hepatic injury. The co-existence of mild sinusoidal fibrosis does not elucidate the successive fibrogenic process hypothesized by Krings et al. (2014). However, the discordance between the restricted pattern of fibrosis and the expanded pattern of activated HSCs observed in the present study points towards the synergism of other cell participants in fibrogenesis.

The importance of our observations lies not only on the assessment of ischemia-related parenchymal findings but also on their diagnostic significance. Liver pathologists are often confronted with the difficulty of diagnosing genuine venous stasis or early NRH, as well as atrophic foci. HSC activation, capillarization of sinusoids and especially K7-positive hepatocytes may serve as a diagnostic tool in favor of a hypoxic lesion. Moreover, the detection of K7-positive hepatocytes may not only be considered a morphological sign of chronic cholestasis but in the appropriate histological context and clinical setting it may be a diagnostically helpful feature of parenchymal ischemia. Immunohistochemical assessment of hypoxia inducible factors (HIF) 1 and 2 could complement the findings of our study in future larger series of cases, including different phases and degrees of ischemia-related conditions.

In conclusion, our findings suggest a hypoxia-induced early reaction of the major cellular components of the liver parenchyma in an effort to create a more resistant microenvironment as a counter-balance to the diminished blood and oxygen supply. The phenotypic alterations may prove invaluable in the differential diagnosis of ischemic liver lesions.

Conflict of interest statement. The authors declare that they have no conflicts of interest

References

Brunt E.M., Neuschwander-Tetri B.A. and Burt A.D. (2012). Fatty liver disease: Alcoholic and non-alcoholic. In: MacSween's Pathology of the Liver. Burt A.D., Portmann B. and Ferrel L. (eds). Churchill Livingstone. Edinburgh. pp 293-359.

Cannito S., Paternostro C., Busletta C., Bocca C., Colombatto S., Miglietta A., Novo E. and Parola M. (2014). Hypoxia, hypoxia-inducible factors and fibrogenesis in chronic liver diseases. Histol. Histopathol. 29, 33-44.

Copple B.L., Bustamante J.J., Welch T.P., Kim N.D. and Moon J.O. (2009). Hypoxia-inducible factor-dependent production of profibrotic mediators by hypoxic hepatocytes. Liver Int. 29, 1010-1021.

DeLeve L.D. (2007). Hepatic microvasculature in liver injury. Semin. Liver Dis. 27, 390-400.

Delladetsima J., Alexandrou P., Giaslakiotis K., Psichogiou M., Hatzis G., Sypsa V. and Tiniakos D. (2010). Hepatic progenitor cells in chronic hepatitis C: a phenomenon of older age and advanced liver disease. Virchows Arch. 457, 457-466.

Delladetsima J.K., Kyriakou V., Vafiadis I., Karakitsos P., Smyrnoff T. and Tassopoulos N.C. (1995). Ductular structures in acute hepatitis with panacinar necrosis. J. Pathol. 175, 69-76.

Desmet V.J. (2011a). Ductal plates in hepatic ductular reactions. Hypothesis and implications. I. Types of ductular reaction reconsidered. Virchows Arch. 458, 251-259.

Desmet V.J. (2011b). Ductal plates in hepatic ductular reactions. Hypothesis and implications. II. Ontogenic liver growth in childhood. Virchows Arch. 458, 261-270.

Hübscher S.G. and Clouston A.D. (2012). Transplantation pathology. In: MacSween's Pathology of the Liver, 6th ed. Burt A.D., Portmann B.C. and Ferrell L.D. (eds). Churchill Livingstone. Philadelphia. pp 853-934.

Józsa L., Réffy A., Demel S. and Szilágyi I. (1981). Ultrastructural changes in human liver cells due to reversible acute hypoxia. Hepatogastroenterology 28, 23-26.

Krings G., Can B. and Ferrell L. (2014). Aberrant centrizonal features in chronic hepatic venous outflow obstruction: centrilobular mimicry of portal-based disease. Am. J. Surg. Pathol. 38, 205-221.

Matsukuma S., Takeo H., Kono T., Nagata Y. and Sato K. (2012). Aberrant cytokeratin 7 expression of centrilobular hepatocytes: a clinicopathological study. Histopathology 61, 857-862.

Michalopoulos G.K., Barua L. and Bowen W.C. (2005). Transdifferentiation of rat hepatocytes into biliary cells after bile duct ligation and toxic biliary injury. Hepatology 41, 535-544.

Nath B. and Szabo G. (2012). Hypoxia and hypoxia inducible factors: diverse roles in liver diseases. Hepatology 55, 622-633.

Pai R.K. and Hart J.A. (2010). Aberrant expression of cytokeratin 7 in perivenular hepatocytes correlates with a cholestatic chemistry profile in patients with heart failure. Mod. Pathol. 23, 1650-1656.

Phillips M.J. (1987). Miscellaneous hepatic conditions. In: The Liver: an Atlas and Text of Ultrastructural Pathology. Phillips M.J. (ed), Raven Press. New York. pp 546-551.

Schön M.R., Kollmar O., Akkoc N., Matthes M., Wolf S., Schrem H., Tominaga M., Keech G. and Neuhaus P. (1998). Cold ischemia affects sinusoidal endothelial cells while warm ischemia affects hepatocytes in liver transplantation. Transplant Proc. 30, 2318-2320.

Stromeyer F.W. and Ishak K.G. (1981). Nodular transformation (nodular "regenerative" hyperplasia) of the liver. A clinicopathologic study of 30 cases. Hum. Pathol. 12, 60-71.

Wanless I.R. (1990). Micronodular transformation (nodular regenerative hyperplasia) of the liver: a report of 64 cases among 2,500 autopsies and a new classification of benign hepatocellular nodules. Hepatology. 11, 787-797.

Wanless I.R. and Huang W.Y. (2011). Vascular Disorders. In: MacSween's Pathology of the Liver. 6th ed. Burt A.D., Portmann B.C. and Ferrell L.D. (eds). Churchill Livingstone. Philadelphia. pp 601-644.

Accepted February 18, 2016